DOI: 10.1002/chem.200801384

Energy Flow in a Purpose-Built Cascade Molecule Bearing Three Distinct Chromophores Attached to the Terminal Acceptor

Anthony Harriman,*[a] Laura Mallon,[a] and Raymond Ziessel*[b]

Abstract: A multicomponent cluster has been synthesised in which four disparate chromophores have been covalently linked through a logical arrangement that favours efficient photon collection and migration to a terminal emitter. The primary energy acceptor is a boron dipyrromethene (Bodipy) dye and different polycyclic aryl hydrocarbons have been substituted in place of the regular fluorine atoms attached to the boron centre. The first such unit is perylene, linked to boron through a 1,4-diethynylphenyl unit, which collects photons in the 320–490 nm region. The other photon collector is pyrene, also connected to the boron centre by a 1,4-diethynylphenyl spacer and absorbing strongly in the 280–420 nm region, which itself is equipped with an ethynylfluorene residue that absorbs in the UV region. Illumination into any of the polycyclic aryl hydrocarbons results in emission from the Bodipy unit. The rates of intramolecular electronic energy transfer have been determined from time-correlated, single-photon counting studies and compared with the rates for Coulombic interactions computed from the Förster expression. It has been necessary to allow for i) a more complex screening potential, ii) multipole–multipole coupling, iii) an extended transition dipole moment vector and iv) bridge-mediated energy transfer. The bridge-mediated energy transfer includes both modulation of the donor transition dipole vector by bridge states and Dexter-type electron exchange. The latter is a consequence of the excellent electronic coupling properties of the 1,4-diethynylphenyl spacer unit. The net result is a large antenna effect that localises the photon density at the primary acceptor without detracting from its highly favourable photophysical properties.

Keywords: boron · electron exchange · energy transfer · fluorescence · photophysics

Introduction

Highly directional electronic energy transfer is an essential feature of natural photosynthesis[1] and it is becoming evermore apparent that such processes will be mandatory for any successful artificial photosynthetic device aimed at converting sunlight into chemical potential.[2,3] Consequently, great attention has been given to the design of molecular arrays containing a well-defined sequence of chromophores that might transfer electronic energy between the terminals.[4] Although the mechanisms for such energy-transfer processes have been understood for many decades, the synthesis of ordered artificial arrays is still at a rather preliminary stage. Many notable achievements have been realised and numerous studies have reported how the dynamics of intramolecular energy transfer relate to the local topology and the nature of the basic constituents.[4] Among the many important contributions to this field, it is pertinent to highlight the engineering of molecular arrays based on tetrapyrrolic pigments as being instrumental in directing photonic energy over relatively large distances under artificial conditions.[5–8] Clearly, many of these systems are bio-inspired and possess the inherent capacity to use the absorbed photon to initiate electron transfer at a remote site.[9] Although most success has been obtained with linear arrays, many unusual molecular architectures have been described that display fast electronic energy transfer[10] and, in several instances, similar events have been characterised for supramolecular

[a] Prof. A. Harriman, L. Mallon
Molecular Photonics Laboratory
School of Natural Sciences
Bedson Building, University of Newcastle
Newcastle upon Tyne, NE1 7RU (United Kingdom)
Fax: (+44) 191-222-8664
E-mail: anthony.harriman@ncl.ac.uk

[b] Prof. R. Ziessel
Laboratoire de Chimie Moléculaire et
Spectroscopies Avancées (LCOSA)
Ecole Européenne de Chimie, Polymères et Matériaux
CNRS, 25 rue Becquerel, 67087 Strasbourg Cedex 02 (France)
Fax: (+33) 3-90-24-26-89
E-mail: ziessel@chimie.u-strasbg.fr

assemblies.[11] These latter systems hold promise for the construction of large light-harvesting units without the need for elaborate covalent synthesis. It should be acknowledged that, at least to some degree, the design of artificial photon collectors has been led by knowledge of the likely energy-transfer mechanism. Thus, the proper positioning of chromophores selected for their optimal spectral overlap integrals is the approved approach for building artificial units operating through the Förster dipole–dipole (i.e., through-space) mechanism. In contrast, close spacing of chromophores linked by conjugated spacer units[12] offers the best chance to construct photon collectors functioning by the Dexter electron-exchange (i.e., through-bond) mechanism. The two mechanisms can act in tandem, especially for triplet-state energy transfer,[13] but the norm is for one mechanism to dominate the proceedings.

Abstract in French: *Une supramolécule originale comportant 4 chromophores distincts liés de façon logique sur une plateforme fluorescente permet de collecter une très vaste gamme de photons et de les faire migrer de façon directionnelle vers un chromophore qui sera le seul émetteur de lumière. L'accepteur d'énergie primaire est une sous-unité Bodipy tandis qu'un ensemble des composés polyaromatiques ont été positionné de telle manière à favoriser le transfert d'énergie. L'ensemble des accepteurs secondaires est lié de façon covalente sur l'atome de bore par l'intermédiaire de triples liaisons qui assurent une très bonne connectivité chimique et électronique. Parmis ces unités, on trouve le 1,4-diéthynylperylène qui collecte les photons dans une plage comprise entre 320 et 490 nm. Un autre collecteur de photons est le 1,6-diéthynylpyrène qui est absorbe entre 280 et 420 nm. Ces deux sous-unités sont liés au bore par un fragment 1,4-diéthynylphényle qui est indispensable pour assurer une synthèse optimale. Enfin un résidu éthynylfluorène permet d'élargir la collection de photons jusqu'à l'ultraviolet lointain et d'assurer une excellente solubilité du composé ciblé. Quelque soit la longueur d'onde d'irradiation utilisée l'ensemble des photons collectés sont transférés vers la sous-unité Bodipy qui fluorescence efficacement. Les vitesses de transfert intramoléculaire d'énergie ont été déterminées par des méthodes traditionnelles de comptage de photons et les vitesses ont été comparées aux valeurs calculées en utilisant les équations de Förster appropriées à une interaction Coulombic. Toutefois il a fallu tenir de nombreux autres facteurs comme: i) un potentiel de surface élargi; ii) de multiple interactions multipole-multipole; iii) un moment de transition dipolaire étendu; et iv) des transferts d'énergie à travers les liaisons. Ce dernier incluant à la fois la modulation du vecteur dipolaire du donneur d'énergie et d'états énergétiques localisés sur l'entretoise ainsi que du double échange d'électron de type Dexter. Ce dernier est du aux excellentes propriétés de couplage électronique au travers de l'entité diéthynylphényle. Le résultat final de ces études est un effet d'antenne étendu, une collection de photon exceptionnelle qui localise toute l'énergie excitonique sur l'accepteur final (le Bodipy) sans perturber ces propriétés optiques et de fluorescence exceptionnelles.*

We have long been interested in maximising the collection efficiency of artificial light harvesters, especially with respect to the energy distribution that can be reaped. In furtherance of this goal, we note that the dipyrromethene framework is especially versatile for synthetic modification, while offering exceptional photophysical and chemical properties.[14,15] Such dyes, usually in the form of boron dipyrromethene (Bodipy) structures, have become extremely popular of late and have formed the basis of numerous opto-electronic devices, sensors, switches and so forth.[16–20] Several Bodipy-based molecular dyads are known to undergo extremely efficient electronic energy transfer under UV illumination, although the transfer distances have been kept short, utilising both Förster and Dexter mechanisms.[21–23] The opportunity to design improved cascade-type arrays centred around Bodipy dyes owes much to the recent introduction of new methodologies for replacement of the B–F bonds,[24] these being an integral feature of conventional Bodipy dyes, with B–aryl or B–ethynyl bonds. Functionalisation through the boron centre opens up facile routes for the design of layered molecular arrays by attaching ancillary light-harvesting units.[25] The most obvious secondary photon collectors are aryl hydrocarbons and we have expanded on previously reported Bodipy-based dyads by the synthesis of new arrays bearing perylene, pyrene and fluorene residues attached by way of the boron centre. The intention is to channel all high-energy photons to the Bodipy-based acceptor in such a way that the photophysical properties of the latter unit are unperturbed by the attachments. The target array should be considered as prototypic of the general approach, since it has already been demonstrated that conventional Bodipy dyes are excellent energy donors[26] for the so-called "expanded Bodipy" dyes that absorb in the far-red region. Once the high-energy side of the photon collector has been optimised, it should be reasonably straightforward to add further layers to the array.

Results and Discussion

Synthesis and characterisation: The target compound comprising separate Bodipy (B), perylene (PE), pyrene (PY) and fluorene (FL) residues, hereafter abbreviated as BPPF, was prepared in five steps from the pre-formed building blocks **1**–**5** as indicated in Scheme 1. The key tenet of the synthetic strategy is the introduction of a polar, protective propargylic function for derivative **3** that facilitates the subsequent purification after cross-coupling to the Bodipy unit (B) and later for the pivotal intermediate BPP. Under such conditions, the target BPPF compound, which is non-polar, can be readily purified by column chromatography, while the absence of contaminants can be checked by ^{1}H NMR spectroscopy. The first step in the overall procedure involves substitution of the two fluorine ligands with 4-ethynyliodobenzene by means of a Grignard derivative. The cross-cou-

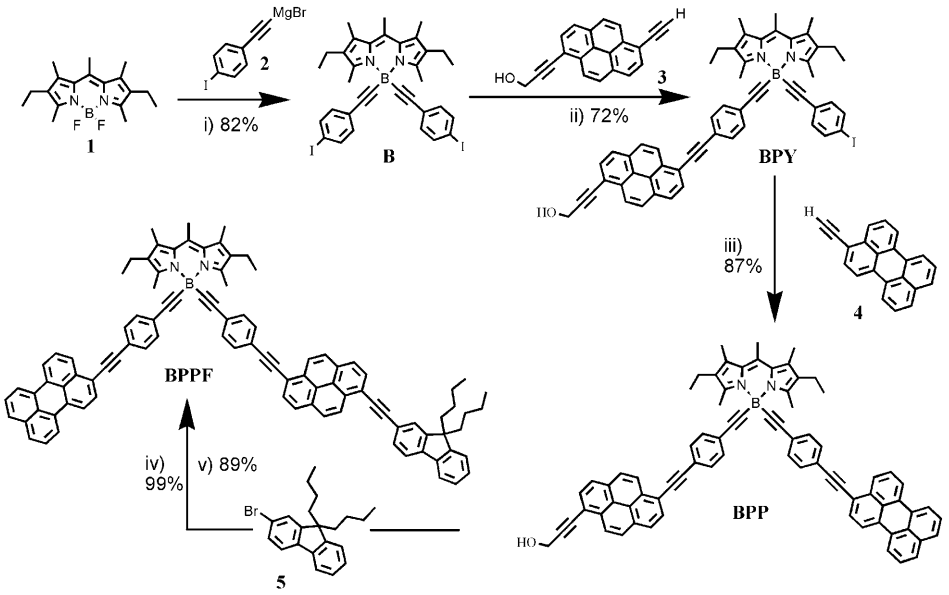

Scheme 1. Keys: i) THF, 60 °C, 1 h; ii) benzene, triethylamine, $[Pd^0(PPh_3)_4]$ 6 mol %, 60 °C, 15 h; iii) benzene, triethylamine, $[Pd^0(PPh_3)_4]$ 6 mol %, 60 °C, 22 h; iv) MnO_2, KOH, THF, 2 h; v) benzene, triethylamine, $[Pd^0(PPh_3)_4]$ 6 mol %, 65 °C, 18 h.

pling reactions between B and **3** and between BPY and **4** are promoted by a Pd^0 catalyst, the course of reaction being followed most conveniently by thin-layer chromatography. The desired deep-orange compounds were isolated by column chromatography on flash silica and recrystallisation was used as a tool to ensure high purity of the final dyes. Removal of the propargylic protective group is achieved using excess MnO_2 in the presence of KOH/THF.

The final step involves cross-coupling of **5** with the unprotected form of BPP, leading to isolation of BPPF in good yield. The chemical structures and molecular compositions of all compounds have been assigned unambiguously on the basis of NMR spectroscopy, mass spectrometry and elemental analysis. A critical fingerprint for the mixed dyes concerns the ^1H NMR spectrum (Figure 1). Thus, equipping the starting dye B with a single ethynylpyrene–propargylic alcohol residue introduces two well-defined singlets at $\delta = 8.55$ and 8.65 ppm, each peak integrates for one proton, located at the *ortho*-position of the ethynylpyrene unit and lying in its deshielding zone (Figure 1b). Additionally, the solitary AB quartet in B is split into two quartets, due to the effect of monosubstitution. The well-resolved singlet seen at $\delta =$ 4.75 ppm and integrating for two protons belongs to the propargylic alcohol residue. Grafting a single ethynylperylene residue to give BPP imports an additional 11 protons that give well-defined patterns in the aromatic region (Figure 1c). This has little influence on the chemical shifts of the two deshielded doublets, thereby confirming their assignment to protons at the *ortho*-position to the ethynyl junction.

It is also notable that the perylene moiety has no significant effect on the chemical shift of the propargylic methylene group. Attaching the di-*n*-butylfluorene unit to the deprotected BPP dye loses the methylene group and the spectrum now appears as a combination of the resonances of the two fragments without pronounced changes in the chemical shifts and coupling constants for either subunit. The linear butyl chains bring a new triplet at $\delta = 2.18$ ppm (integration for 4H), due to the methylene groups in close proximity to the five-membered ring, and additional peaks below $\delta = 1$ ppm (Figure 1d). Although asymmetry is introduced by the presence of two disparate polycyclic aromatic residues in several of these new dyes, the methyl groups at the lower rim of the Bodipy unit are little affected. The number of quaternary ethynyl carbon atoms, however, increases by importing each new ethynyl fragment and is a convenient marker for the status of synthetic progress. For example, BPPF exhibits eight separate C≡C resonances in the $\delta = 96.8$–88.6 ppm range.

Photophysical properties of the target molecule BPPF: The absorption spectrum recorded for BPPF in common organic solvents shows a large number of transitions in the range from 200–550 nm, which can be assigned on the basis of spectra measured for the various reference compounds (Scheme 2). The lowest energy transition is well resolved at 515 nm (Figure 2) and corresponds to the 0–0 transition associated with population of the first-excited singlet state of the Bodipy unit.[27] This transition, together with its set of vibrational satellites, is essentially unperturbed relative to the reference compound. The corresponding transition to the second-excited singlet state, seen for the reference compound as a broad, relatively weak band centred at 370 nm,[28] cannot be observed for BPPF because of overlapping transitions localised on the auxiliary chromophores. Lying at slightly lower energy than the S_0–S_1 transition associated with the Bodipy unit are bands due to localised π–π* transitions on the ethynylperylene (PE) unit.[29] The lowest energy of the PE-based bands lies at 476 nm and is again accompanied by an envelope of vibrational fine structure. The series of π–π* transitions localised on the ethynylpyrene (PY) chromophore is evident at higher energies,[30] clearly overlapping with the S_0–S_2 transitions associated with the PE unit, and has its 0–0 band centred at 441 nm. Finally, the group of π–π* transitions related to the fluorene unit[31] are difficult to resolve from bands associated with the other chromophores, but, by careful comparison to the reference compound, the 0–0 band can be identified at 305 nm. The absorption spectrum is hardly affected by changes in solvent

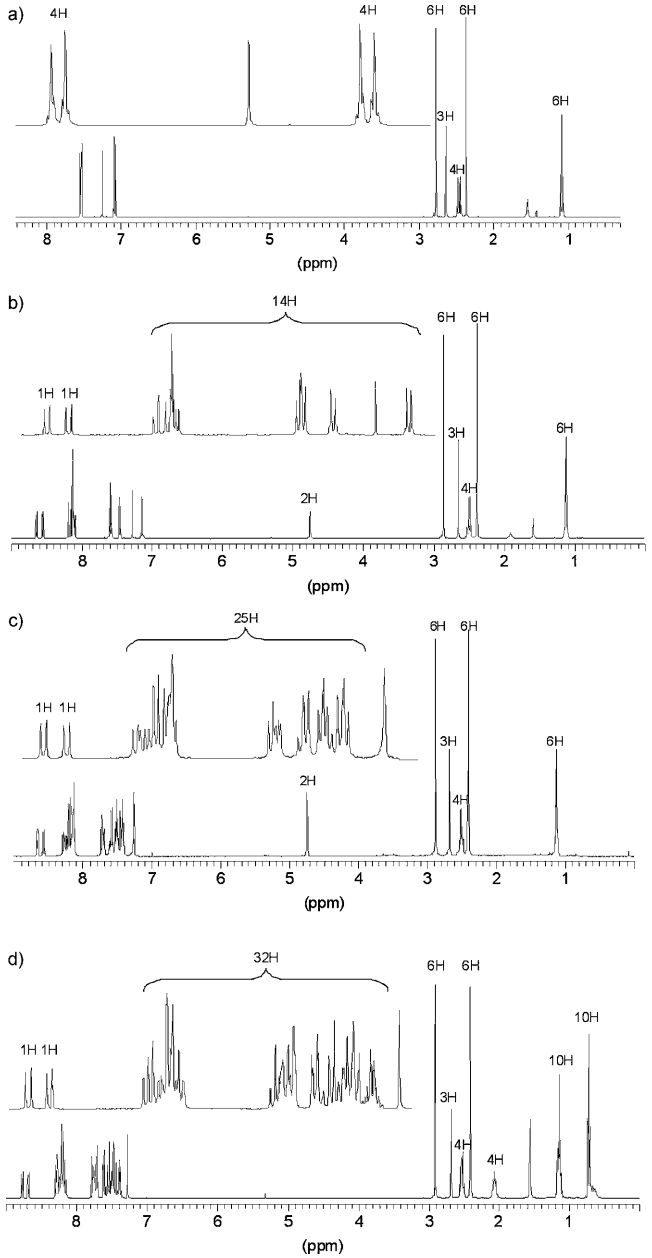

Figure 1. Proton NMR (400.1 MHz) spectra measured in $CDCl_3$ at room temperature; a) B, b) BPY, c) BPP and d) BPPF.

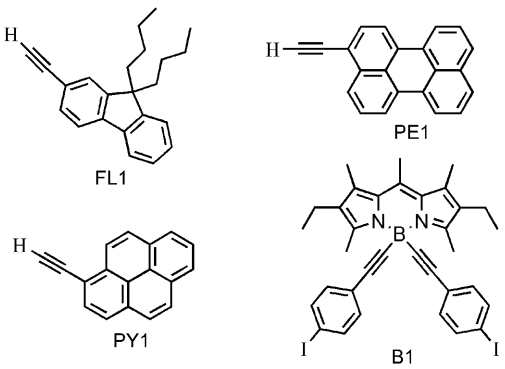

Scheme 2. Formulae of the various reference compounds used to calculate the Förster-type properties.

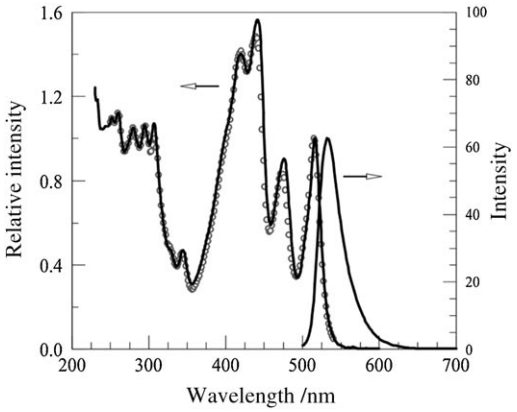

Figure 2. Overlap of absorption (solid curve) and excitation (circles) spectra recorded for BPPF in CH_2Cl_2 and the corresponding fluorescence spectrum observed following excitation at 500 nm.

polarity and is well preserved on dispersing BPPF in polymeric media. The entire spectrum appears as a superimposition of spectra recorded for the relevant reference compounds and there are no evident signs of strong electronic coupling between the subunits.

Fluorescence can be detected from BPPF following illumination with near-UV light (Figure 2). The emission profile and maximum correspond very well with those recorded for the Bodipy reference compound (B1) and it is clear that this unit is primarily responsible for the emission observed in fluid solution. The Stokes' shift is only 660 cm^{-1}, while the vibrational pattern, which consists of four equally spaced bands of common half-width (FWHM = 535 cm^{-1}), closely resembles that found for B1. Furthermore, the corrected excitation spectrum matches very well with the absorption spectrum recorded over the range from 250 to 520 nm (Figure 2) and it is clear that the majority (i.e., >90%) of all photons absorbed by BPPF result in fluorescence from the Bodipy moiety. In CH_2Cl_2 at room temperature, the fluorescence quantum yield (ϕ_F) is 0.62, for excitation at 495 nm, while the excited-singlet state lifetime (τ_S), recorded by time-correlated, single-photon counting, was found to be 6.3 ns. Time-resolved fluorescence decay curves recorded for BPPF following excitation at 495 nm are strictly mono-exponential. These derived photophysical values remain comparable to those recorded for B1, except that the measured ϕ_F seems slightly lower for BPPF than for the simpler analogue. Notably, the radiative rate constant ($k_{RAD} = 1 \times 10^8$ s^{-1}) derived from the experimental data appears to be consistent with those found[25,26] for several other B–ethynyl substituted Bodipy dyes. The overall conclusion raised by this phase of the work, therefore, is that efficient, intramolecular electronic energy transfer takes place from the polycyclic aryl hydrocarbons to Bodipy.

Other fluorescence bands are apparent in the emission spectrum, according to the choice of excitation wavelength, which correspond to residual fluorescence from the ancillary chromophores (Figure 3). This residual fluorescence occurs with rather low quantum yield, although the overlapping ab-

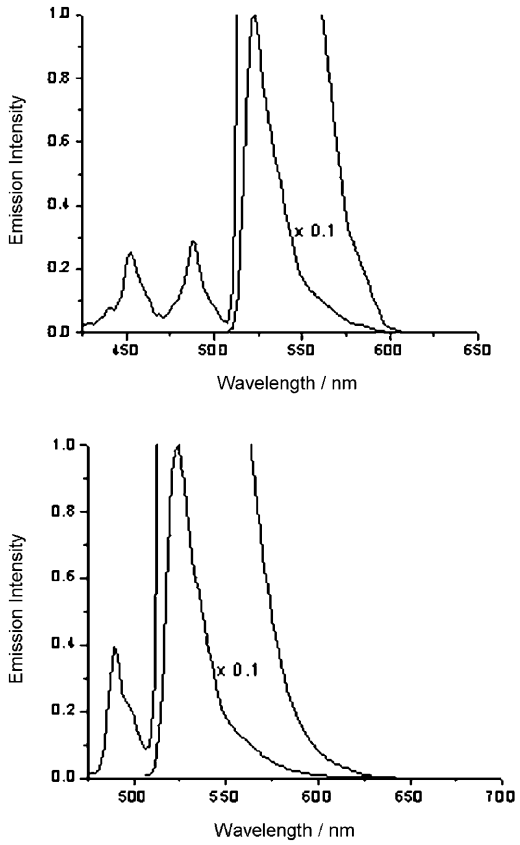

Figure 3. Fluorescence spectra recorded for BPPF in a rigid glass at 77 K following excitation into the PY subunit at 392 nm (upper panel) and into the PE subunit at 460 nm (lower panel).

sorption bands render accurate determination of the respective ϕ_F values a hazardous task. This was attempted by comparing the emission properties recorded for BPPF in CH_2Cl_2 with those measured for an equimolar mixture of the reference compounds, after matching the absorbance values at appropriate excitation wavelengths and assuming that the mixture is free of intermolecular quenching. The net findings give a crude indication of the level of residual emission from each polycyclic aryl hydrocarbon. The results can be conveniently expressed in the form of a residual fluorescence probability (P_F), defined by the ratio of integrated fluorescence yields for subunit X in BPPF compared to that unit in the mixture and converted to percentage. Furthermore, by comparison to the fluorescence quantum yield of the particular reference compound (ϕ_F^{REF}), an estimate can be made of ϕ_F for the subunit in BPPF (Table 1). According to this rough analysis, the residual fluorescence from both pyrene and perylene units amounts to about 1% of the emission characteristic of PY1 and PE1 respectively. It is difficult to make a realistic estimate for the fluorene subunit, because of the uncertainty relating to the number of photons absorbed by this moiety, but it is clear that, at best, the residual emission is only a small fraction ($<0.5\%$) of that from the reference compound, FL1. Time-resolved fluorescence studies support these general findings in as much

Table 1. Comparison of fluorescence quantum yields and lifetimes recorded for the reference compounds and the various subunits present in BPPF.[a]

Property	Bodipy (B1)	Perylene (PE1)	Pyrene (PY1)	Fluorene (FL1)
ϕ_F^{REF}[b]	0.28	0.63	0.86	0.95
τ_S^{REF} [ns]	6.4[b]	4.1[c]	21.0[d]	1.7[e]
P_F [%]	NA	1.3	0.7	0.1
$\phi_F(X)$[f]	NA	0.008	0.006	0.001
τ_S [ps][g])	NA	44	55	<30
τ_S [ps][h]	NA	53	125	2

[a] Measured in CH_2Cl_2 at 20 °C. [b] Refers to B1. [c] Refers to PE1. [d] Refers to PY1. [e] Refers to FL1. [f] Refers to the estimated fluorescence quantum yield of subunit X in BPPF. [g] Refers to the fluorescence lifetime of subunit X in BPPF, measured by TC-SPC. [h] Fluorescence lifetime of subunit X in BPPF anticipated from the relative fluorescence yields.

as the lifetime anticipated on the basis of the residual fluorescence is in fair agreement with that determined experimentally (Table 1).

The fluorescence spectral properties of BPPF were also measured in a methyltetrahydrofuran (MTHF) glassy matrix at 77 K. Here, all the individual emission bands are sharpened and slightly blue-shifted relative to those recorded at room temperature, but similar behaviour is apparent (Figure 3). Thus, fluorescence from the fluorene unit was difficult to resolve from the background and could not be supported by a meaningful excitation spectrum. Fluorescence from the Bodipy unit was readily observed with a maximum at 525 nm (Figure 3). This is the only emission peak observed when the sample is illuminated at 495 nm. Direct excitation into the perylene subunit at 460 nm results in strong fluorescence from Bodipy together with weak PE-based emission centred at 490 nm (Figure 3). Excitation at 392 nm at which both pyrene and perylene subunits absorb results in strong fluorescence from the Bodipy unit and weak emission from both PE and PY chromophores. This last fluorescence signal is centred at 453 nm (Figure 3).

It is notable that fluorescence from the polycyclic aryl hydrocarbons is somewhat more pronounced with respect to that from Bodipy at 77 K than at room temperature, indicating that energy transfer is very slightly activated. In each case, excitation spectra confirmed that PE- and PY-based emission arises from that chromophore, while Bodipy-based fluorescence is the consequence of energy transfer, unless the Bodipy chromophore is excited directly. Close examination of the excitation spectral profile for the PE-based fluorescence shown in Figure 3 indicates that there is little, if any, energy transfer from the PY-based chromophore, despite the favourable overlap integral (see below).

Excitation into the individual subunits: Selective illumination into the fluorene subunit is fraught with experimental difficulties and it has not been possible to properly resolve fluorescence from this moiety. Our best estimate for the fluorescence lifetime of the fluorene unit in BPPF places it at less than 30 ps, following excitation at 266 or 317 nm.

Comparison to FL1[32] indicates that the rate constant for electronic energy transfer (k_{EET}) must exceed $3\times10^{10}\,s^{-1}$ under these conditions. Energy transfer, therefore, can be considered as being quantitative. Given the close proximity to the pyene unit, and the almost ideal orientation factor, it seems unnecessary to consider very long-range Förster energy transfer from FL to either perylene or Bodipy units. Consequently, we restrict attention to energy transfer to the nearby pyrene unit. Furthermore, the ethynyl linkage provides an efficient conduit for through-bond electron exchange[33] and there seems little doubt that bridge-mediated energy transfer[34] will contribute to the overall process. An evident problem for this system concerns defining whether the FL–PY pair acts as two separate reactants or as a single delocalised entity.[22] Calculations carried out at the DFT B3LYP/6-31G* level suggest that two units act as independent chromophores, but there is no barrier to rotation around the connector and it should be assumed that the presence of the second chromophore will influence the electronic properties of the first unit.

The situation is much easier for the perylene subunit, for which the spectroscopic energy gap between singlet states localised on perylene and Bodipy units is approximately 1590 cm^{-1}. This is too high for the two excited states to exist in thermal equilibrium at ambient temperature. No other energy-transfer routes need be considered. Steady-state fluorescence spectroscopy shows that there is a small amount of residual fluorescence from the PE unit. An excitation spectrum recorded for this residual mission confirms that it arises from the perylene unit and that it is not a consequence of slow energy transfer from pyrene. The lifetime ($\tau_S=40$ ps) of this residual emission was close to the limit of that measurable by our time-correlated, single-photon counting set-up, especially because the range of emission wavelengths is fairly narrow, but a second estimate could be obtained by monitoring the growth of fluorescence localised on the Bodipy acceptor after excitation into the PE-based chromophore at 473 nm (Figure 4). The globally averaged lifetime for the S_1 state associated with the perylene subunit was found to be 44 ± 4 ps (Table 1); note that we cannot rule out the possibility of a faster component in the decay records, given the somewhat limited temporal resolution, but there are no indications for such behaviour. The same lifetime was observed following excitation at 440 nm and for analysis over a modest range of emission wavelengths. The derived lifetime compares reasonably well with that projected on the basis of the residual fluorescence noted from the steady-state measurements (Table 1). The experimental rate constant for electronic energy transfer (k_{EET}), measured from the time-resolved fluorescence profiles following excitation at 473 nm, can now be established as being $2.3\times10^{10}\,s^{-1}$.

Excitation at 390 nm represents the best compromise for selective illumination into the pyrene unit, although it should be stressed that both Bodipy and perylene subunits absorb at this wavelength. It has already been shown that, under these conditions, weak PY-based fluorescence can be

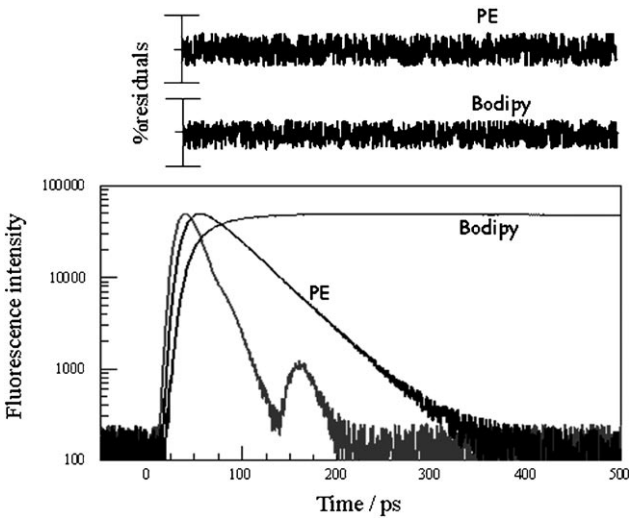

Figure 4. Time-resolved fluorescence decay curves recorded following selective excitation into the perylene subunit at 473 nm. Individual curves refer to the instrumental response function (gray line) and decay curves recorded at 495 nm (PE) and 565 nm (Bodipy). The upper panels show the respective percentage residuals after deconvolution and least-squares analysis; the marks represent $\pm0.5\,\%$ deviation.

seen at both 77 K and room temperature (Figure 3), but that the yield of this emission is severely reduced relative to that of a non-interacting mixture of chromophores (Table 1). Time-resolved fluorescence studies indicate that the first-excited singlet state of pyrene in BPPF has a lifetime of only 55 ± 5 ps compared to 21 ns found for the isolated reference compound (Figure 5). The decay profile recorded for residual PY-based emission follows first-order kinetics. Quenching is due to electronic energy transfer to Bodipy; this was con-

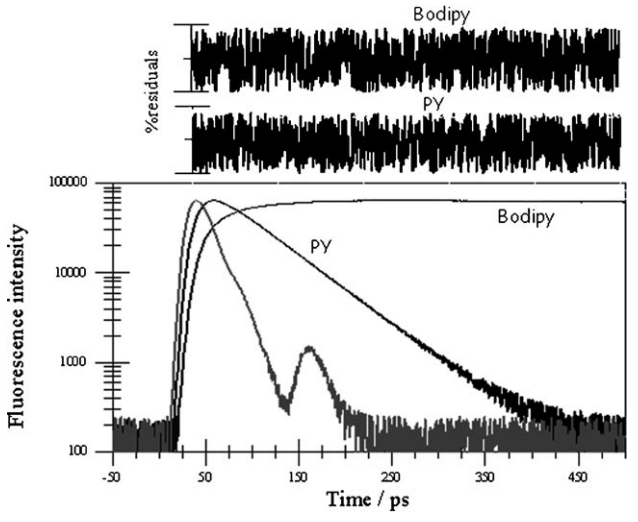

Figure 5. Time-resolved fluorescence decay curves recorded following selective excitation into the pyrene subunit at 390 nm. Individual curves refer to the instrumental response function (gray line) and decay curves recorded at 450 nm (PY) and 565 nm (Bodipy). The upper panels show the respective percentage residuals after deconvolution and least-squares analysis; the marks represent $\pm0.6\,\%$ deviation.

firmed by monitoring growth of Bodipy-based fluorescence following excitation at 390 nm and the experimentally determined rate constant (k_{EET}) is 1.8×10^{10} s^{-1}.

There is strong spectral overlap between emission from the PY unit and absorption by the PE unit such that we need to consider Förster-type energy transfer from pyrene to perylene. Clearly, in this case there will be no bridge-mediated energy transfer. However, excitation spectra do not support the idea of PY–PE energy transfer. Monitoring PE-based fluorescence after excitation into the PY chromophore, but recalling that absorption is not fully selective, shows no slow growth of the perylene emission. We conclude, therefore, that energy transfer from PY to Bodipy is the major route for deactivation of the S_1 state localised on pyrene.

Calculation of the Förster rate constants: The experimentally determined rate constants for intramolecular electronic energy transfer (k_{EET}) are collected in Table 2. These values

Table 2. Summary of parameters associated with Förster-type energy transfer between the various subunits in BPPF, as obtained for a static system and assuming only dipole-dipole interactions.

Reactant pair	J_F [10^{-14} mmol^{-1} cm^6]	R_{CC} [Å]	$\langle\kappa\rangle^2$	k_F [10^9 s^{-1}]	k_{EET} [10^9 s^{-1}]
FL–PY	2.7	10.0	2.97	14000	>30
FL–PE	0.25	33.1	0.81	0.27	NA
FL–Bodipy	0.38	24.5	0.010	0.03	NA
PY–Bodipy	0.73	14.6	0.022	0.21	18
PY–PE	2.9	24.6	0.91	1.5	NA
PE–Bodipy	9.1	15.6	0.006	2.0	23

can now be compared with calculated rate constants for Förster-type energy transfer between the various subunits. There is, however, growing awareness that conventional Förster theory, as developed for widely spaced reactants,[35] is not applicable to reactants held in close proximity by a bridge,[36] especially if the latter comprises conjugated units.[37] Consequently, we have made the comparison between observed and calculated rate constants at several levels, each intended to correct for specific issues relating to the transfer process. First, we calculate the rate constants (k_F) for Förster-type dipole–dipole energy transfer assuming a static system. These k_F values, in fact, are readily computed from Equation (1) in which ϕ_F and τ_S refer to the fluorescence quantum yield and lifetime of the appropriate reference compound, respectively, for the donor and s is the screening potential of the surrounding medium, often equated to the reciprocal of the square of the solvent refractive index (n^{-2}).[38] In the case of intramolecular energy transfer between closely spaced reactants it is far from evident that this simple expression will give an adequate representation of the screening of the respective dipoles and we have opted for the more complex expression included in Equation (1).[39] This simple modification leads to a 40% increase in the calculated k_F values. The spectral overlap integral,[35] J_F, refers to overlap between the absorption spectrum of the acceptor ($\varepsilon_A(\nu)$) and the normalised reduced emission spectrum of the donor ($F_D(\nu)\nu^{-3}$); again, the reference compounds were used to calculate these values and representative overlap integrals are illustrated in Figure 6. It is notable

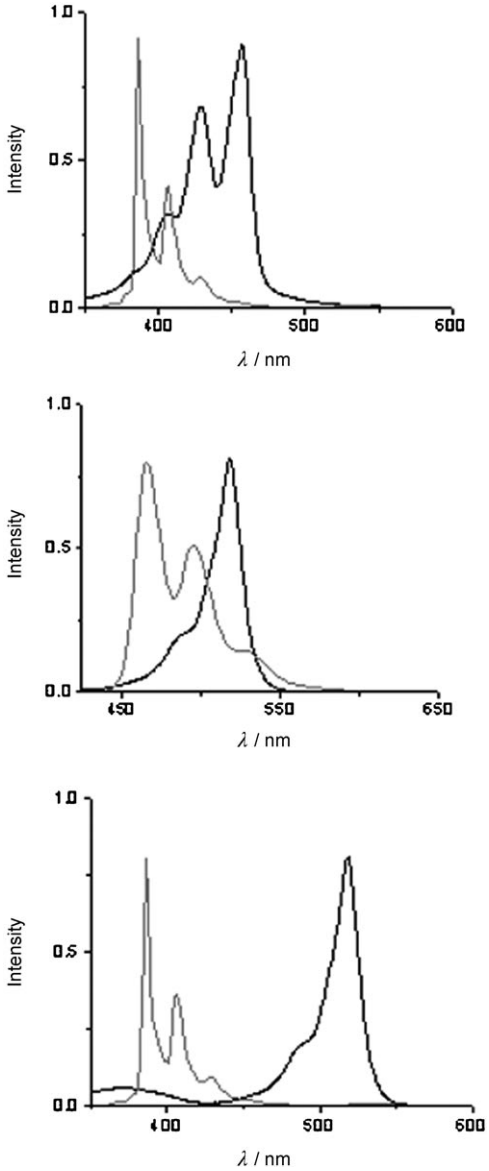

Figure 6. Illustrations of selected spectral overlap integrals: FY–PE (upper panel), PE–Bodipy (centre panel) and PY–Bodipy (lower panel).

that emission from pyrene overlaps with the S_0–S_2 absorption transition localised on Bodipy, whereas fluorescence from perylene overlaps with the corresponding S_0–S_1 absorption transition. The average centre-to-centre separations (R_{CC}) were obtained from energy-minimised computer models. Each of the derived values is listed in Table 2 and specified according to which pair of reactants is under consideration.

$$k_{F'} = \frac{8.8 \times 10^{-25} s^2 \phi_F \kappa^2}{\tau_s R_{CC}^6}$$

$$J_F = \frac{\int_0^\infty F_D(\nu)\varepsilon_A(\nu)\nu^{-4}d\nu}{\int_0^\infty F_D(\nu)d\nu} \quad (1)$$

$$s = \frac{3}{(2n^2+1)}$$

The remaining term in the Förster expression[38] is the orientation factor (κ), which refers to the alignment of transition dipole moments on the donor and acceptor units[40] and it is this term that is subject to the greatest amount of uncertainty because of conformational motion. Values for κ can be computed readily from Equation (2) in which θ_D and θ_A are the angles between the transition dipole vectors of the donor and acceptor, respectively, with the molecular axis and ϕ_{DA} is the angle between the two dipole moment vectors. Information about these vectors was sought from transition-density profiles made for the target compound BPPF. There is, in fact, little difficulty to compute κ for the fluorene–pyrene pair for which the mean value, $\langle\kappa\rangle^2$, is close to 3 (Table 2). For the other pairs, κ^2 is kept rather small by the poor alignment of the transition density vectors (Table 2); the main problem being that the transition density for Bodipy lies along the long axis of the chromophore and is almost orthogonal to that of the substituent. The net result is that the computed k_F values are very much reduced relative to the experimental values, at least for the cases in which Bodipy acts as the acceptor.

$$\kappa^2 = (\sin\theta_D \sin\theta_A \cos\phi_{DA} - 2\cos\theta_D \cos\theta_A)^2 \quad (2)$$

The conventional solution to cases for which k_F falls well short of the experimental rate constant is to attribute the difference to a competing electron-exchange process. Prior to doing so, however, it is prudent to ensure that higher order multipoles are included in the calculation of the overlap integral[41] and that static $\langle\kappa\rangle$ values are replaced with parameters that take into account structural fluctuations.[42] Allowing for dipole–quadrupole and quadrupole–quadrupole interactions[43] is important for short-range Coulombic effects and is easily accommodated for BPPF. According to the results of a series of molecular dynamics simulations (MDS), BPPF is not a rigid molecule and, in addition to the evident rotations, undergoes considerable bending and twisting motions around the connecting diethynylene–benzene functions. Such behaviour has been noted before and leads to conformational heterogeneity on the time scale of fluorescence measurements.[25,26] These internal motions do not seriously affect the centre-to-centre separation distances (R_{CC}) between the various subunits, except for the pyrene–perylene pair, but do disturb their relative orientations. As a consequence, computation of k_F has to take into account the likely distribution of orientations. This situation is illustrated below for the pyrene–perylene pair.

Thus, the MDS runs, carried out in a reservoir of water molecules, were used to track the PY–PE separation distance over a reasonable time period (Figure 7, upper panel).

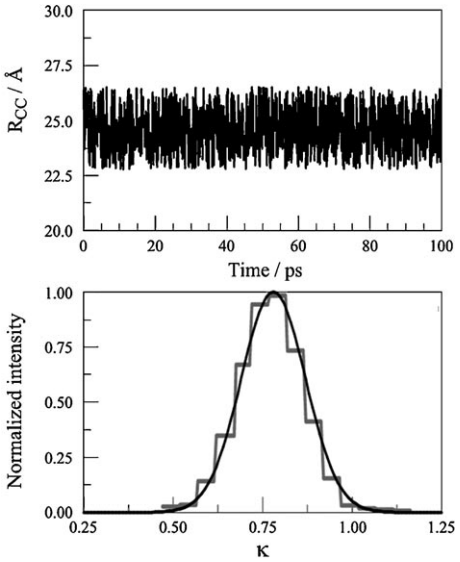

Figure 7. Upper panel: Evolution of the center-to-center separation distance between the pyrene and perylene units in BPPF as determined from MDS runs. Lower panel: Orientation factor κ^2 determined for the various geometries sampled during the MDS runs; the steps refer to the frequency of κ^2 values determined by MDS and the solid black curve represents a Gaussian fit to the data.

The average R_{CC} value is given in Table 2, while the smallest and largest separations, respectively, are 22.5 and 27.0 Å. These data were categorised in terms of frequency of occupancy so that the κ value could be computed for each R_{CC} value and presented in the form of a histogram (Figure 7, lower panel). The mean κ^2 value falls from 0.91 to 0.78 in this way. Rotation around the connecting ethyne-based bridge does not affect the computed κ^2 value, but variations in the angle at the B centre cause a modest perturbation in the mean κ^2 value. The net result of these considerations based on the MDS runs and allowing for the multipole–multipole interactions is that the projected k_F value falls slightly from 1.5×10^9 s^{-1} for the static system to 1.4×10^9 s^{-1} for dynamic behaviour. Similar MDS studies were made for the other couples and revised k_F values were calculated, after allowance for both dipole and quadrupole interactions. The main results are compiled in Table 3. It is seen that in those

Table 3. Summary of parameters associated with Förster-type energy transfer between the various subunits in BPPF, as obtained for a dynamic system and allowing for multipole–multipole interactions.

Reactant pair	$\langle\kappa\rangle^2$	k_F [10^{10} s^{-1}]	V_{DA} [cm^{-1}]	J_{DA} [10^4 cm]	V_{CO} [cm^{-1}]
FL–PY	2.75	2000	>30	2.9	>7
PY–Bodipy	0.15	0.17	11.8	1.2	3.4
PY–PE	0.78	0.14	NA	3.1	2.4
PE–Bodipy	0.08	3.1	5.2	7.8	7.4

cases in which Bodipy functions as the acceptor, k_F is significantly increased relative to the corresponding value calculated for the static system. Furthermore, the revised k_F value for the perylene–Bodipy pair is now rather close to the experimental value. The revised k_F value for the pyrene–Bodipy couple, however, still falls well short of the experimental value. In part, this problem lies with the reference compound PY1 being unable to properly represent the overlap integral, but using the emission profile from the PY unit in BPPF, although this is very weak, does not increase the calculated k_F value by more than a factor of twofold. In making these revised calculations of k_F we have used the histogram data for κ^2 as input and computed individual rate constants normalised by the occupation frequency. The quoted k_F value is the sum of the individual rates.

The final point to consider with respect to the Coulombic mechanism relates to the possibility of bridge-mediated energy transfer.[44] This process is not to be confused with Dexter-type electron exchange,[45] but refers specifically to the effect that a conjugated bridge might have on the electronic properties of the donor. For BPPF, the bridge connecting the PY and PER donors to the Bodipy acceptor is a diethynylated benzene unit and, in reality, it is difficult to assign the boundary between donor and bridge. This is an even bigger problem for the FL–PY couple. Computational studies made at the DFT B3LYP/6-31G* level indicate that the phenyl ring in the bridge lies orthogonal to the plane of the aryl polycycle for both PY and PE, while the PY and FL units are also orthogonal in the FL–PY dyad, at least for the lowest energy conformations for the ground state. Rotation around the connecting ethyne unit is facile, however, and serves to increase the degree of π-orbital conjugation. This effect is shown in Figure 8 for the PE unit, and is similar for the other chromophores. The transition density is spread over the perylene-based chromophore, but does not involve the phenyl ring in the bridge. For the corresponding coplanar geometry, the computed transition density profile stretches onto the phenyl ring. The net result is an extension of the transition dipole for the chromophore, a small change in the corresponding vector and a marked reduction in the donor–acceptor separation. Indeed, this separation is now considerably less than the sum of the diameters of the donor and acceptor units and this will have important consequences for the attempted application of Förster theory. A direct consequence of this behaviour is that dipole–quadrupole and quadrupole–quadrupole interactions outweigh dipole–dipole interactions at short separations.

We can represent the overall rate constant for electronic energy transfer (k_{EET}) in the form of Equation (3), in which V_{DA} is the electronic coupling matrix element and J_{DA} is a revised form of the spectral overlap integral,[46] with units of cm, according to Equation (4). In this case, the individual spectral curves are normalised. Now, the overall V_{DA} term can be split into Coulombic (V_{CO}) and exchange (V_{EX}) terms. The Coulombic matrix element can be expressed in the form of Equation (5), in which κ is the orientation factor, allowing for multipole–multipole interactions, and d_D and d_A are the transition dipole moments for donor and acceptor, respectively.[47] In principle, it is possible to compute[48] a value for V_{EX}, but this is outside the scope of the present study. Instead, we can attempt to allow for the bridge-mediated effects by making use of Equation (5).

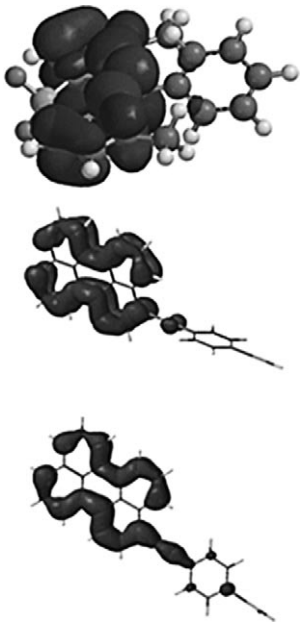

Figure 8. Transition density plots for the Bodipy chromophore (upper panel) and for the perylene-based chromophore in the lowest-energy conformation (centre) and after rotation of the bridging phenyl ring (lower panel).

$$k_{EET} = \frac{|V_{DA}|^2 J_{DA}}{\hbar^2 c} \tag{3}$$

$$J_{DA} = AB \int \frac{f_D(\nu)}{\nu^3} \frac{\varepsilon_A(\nu)}{\nu} d\nu$$
$$A \int \frac{f_D(\nu)}{\nu^3} d\nu = B \int \frac{\varepsilon_A(\nu)}{\nu} d\nu = 1 \tag{4}$$

$$V_{CO} = \frac{s\kappa}{4\pi\varepsilon_0} \frac{|d_D||d_A|}{R^3} \tag{5}$$

Thus, values for the total electronic coupling matrix element, V_{DA}, were determined from Equation (3) by using the spectroscopic data to evaluate J_{DA} (Table 3). Spectroscopic data were also used[49] to calculate values for d_D and d_A; the derived values being 1.6, 2.0, 7.5 and 4.5 D for the FL, PY, PE and Bodipy chromophores, respectively. These data were then used, in conjunction with the mean κ^2 values determined by MDS, to compute the coupling constants for Coulombic interactions, V_{CO}. These V_{CO} values should contain all the various correction terms for Coulombic effects and, therefore, are taken to represent the full extent of the through-space energy transfer. By difference, we obtain estimates of the coupling element for electron exchange, V_{EX}. Several interesting points now emerge. Firstly, we say little

about the mechanism for energy transfer in the FL–PY pair. Secondly, electron exchange accounts for about 50% of the overall energy-transfer processes for the PE–Bodipy couple. For the PY–Bodipy couple, in which the spectral overlap involves the S_2 state on the Bodipy-based acceptor, the electron-exchange mechanism accounts for about 90% of the total transfer. The computed V_{CO} values are reasonably comparable for energy transfer from PY to Bodipy and PE to Bodipy, but there is a major disparity in the V_{EX} values for these two couples. This might be due to the much higher energy of the PY-based donor, since this will favour superexchange type coupling with bridge states. Finally, the calculations predict quite appreciable Coulombic coupling between PY and PE chromophores, for which there can be no electron exchange. It is now clear that the reason this energy-transfer step is not seen experimentally is because of the efficient electron exchange interactions between PY and Bodipy.

Conclusions

The cascade-type system described herein is a major advance on earlier prototypes in which a Bodipy-based dye was attached to an auxiliary photon collector to form a molecular dyad or triad.[21,22,24,25] Several such systems have been studied, including dyads equipped with expanded Bodipy units that absorb and emit in the far-red region.[26] The multicomponent BPPF array absorbs across a relatively wide spectral window and transfers absorbed photons to the emissive Bodipy unit with high efficiency, even at 77 K and in a plastic film. It has been possible to measure rate constants for two of the key steps, although transfer from fluorene to pyrene is too fast to be observed under our conditions. The net effect is to produce an improved solar concentrator[50] that is highly versatile and suitable for further expansion. In many respects, the successful isolation of BPPF relies on the ability to synthesise asymmetrical derivatives in which the B–F bonds are replaced with B–C analogues, which might be identical or disparate according to the needs of the experiment. This synthetic protocol creates the opening by which to generate a vast library of next-generation photon collectors from pre-formed molecular modules. In the case of BPPF, the terminal acceptor maintains a relatively long excited-state lifetime and a high fluorescence quantum yield.

An additional feature of BPPF is the use of diethynylbenzene connectors. This is a common spacer unit that provides excellent through-bond electron exchange for both singlet and triplet energy transfer.[51] It provides strong electronic coupling between Bodipy and both perylene- and pyrene-based residues, but without promoting adiabatic coupling. Consequently, the individual subunits retain their own identity whilst undergoing rapid electronic energy transfer. Both dipole–dipole[32] and electron exchange[34] mechanisms are believed to operate simultaneously. This situation improves the light-harvesting properties. It is worth pointing out that the apparently unfavourable orientation factor for dipole–dipole transfer is improved markedly by structural fluctuations around the spacer groups. This mechanism provides an alternative route in the event that photochemical damage destroys the through-bond process along one of the arms. The optimum example of this insurance scheme would come into play should the link between pyrene and Bodipy become insulating. In this case, dipole–dipole energy transfer from pyrene to perylene would ensure that the photon flow remained uninterrupted. Such eventualities, although not proven in this case and not exactly coming under the banner of molecular self-repair, are likely to become an essential part of future molecular-scale opto-electronic devices as a means to offset damage by singlet molecular oxygen.

Experimental Section

Synthesis: The 400.1 (^{1}H) and 100.3 (^{13}C) MHz NMR spectra were recorded at room temperature with perdeuterated solvents as internal standards: δ(H) is quoted in ppm relative to residual protiated solvent and δ(C) is given in ppm relative to the solvent. FT–IR spectra were recorded on the neat liquids or as thin films prepared with a drop of dichloromethane and evaporated to dryness on KBr pellets. Chromatographic purification was conducted using standardised flash-silica gel. Thin-layer chromatography (TLC) was performed on aluminium oxide or silica plates coated with fluorescent indicator. All mixtures of solvents are given as volume/volume (v/v) ratios. Tetrahydrofuran was distilled over sodium and benzophenone. Samples of 4,4-difluoro-1,3,5,7,8-pentamethyl-2,4-diethyl-4-bora-3a,4a-diaza-s-indacene (**1**),[52] 1-ethynyl-8-propargylicalcoholpyrene (**3**),[53] 3-ethynylperylene (**4**),[54] and 2-bromo-9,9-di-*n*-butyl-9H-fluorene (**5**),[55] were prepared and purified according to literature procedures. All reactions were carried out under argon using Schlenk-tube and vacuum-line techniques.

Compound B: A Schlenk flask was charged with the 1-ethynyl-4-iodobenzene (**2**; 510 mg, 2.23 mmol) and anhydrous THF (10 mL). A solution of ethylmagnesium bromide (2.1 mL, 2.15 mmol, 1 M in THF) was added dropwise and the mixture was stirred at 60 °C for 2 h. The resulting solution was transferred at room temperature through a cannula to a solution of **1** (285 mg, 0.90 mmol) in anhydrous THF (15 mL). The mixture was stirred at 60 °C for 1 h. After cooling to room temperature, the solvent was removed by rotary evaporation. The residue was treated with water and extracted with dichloromethane. The organic phases were washed with water and dried over absorbent cotton. The solvent was removed by rotary evaporation. The residue was purified by chromatography on silica gel, eluting with dichloromethane/petroleum ether (v/v 5:95) to give 540 mg (82%) of B as a deep-orange solid. ^{1}H NMR ($CDCl_3$): $\delta = 7.54$ (d_{AB}, $^3J = 8.1$ Hz, 4H), 7.08 (d_{AB}, $^3J = 8.1$ Hz, 4H), 2.77 (s, 6H), 2.64 (s, 3H), 2.47 (q, $^3J = 7.7$ Hz, 4H), 2.37 (s, 6H), 1.08 ppm (t, $^3J = 7.7$ Hz, 6H); ^{13}C {^{1}H} NMR ($CDCl_3$, 100 MHz): $\delta = 152.2$, 140.2, 137.4, 135.0, 133.6, 133.0, 130.5, 125.4, 92.8, 17.8, 17.7, 15.4, 15.1, 14.3 ppm; ^{11}B NMR (128.4 MHz, $CDCl_3$): $\delta = -9.85$ ppm (s); IR (KBr): $\tilde{\nu} = 3057$ (m), 2965 (m), 2934 (m), 2166 (m), 1604 (s), 1565 (s), 1487 (s), 1389 (m), 1364 (m), 1324 (m), 1187 (s), 1067 (m), 1056 (m), 846 cm^{-1} (m); EI-MS: *m*/*z* (%): 734.1 (100) $[M]^+$; elemental analysis calcd (%) for $C_{34}H_{33}BI_2N_2$ (M_r = 734.26): C 55.62, H 4.53, N 3.82; found: C 55.45, H 4.36, N 3.68.

General procedure for the cross-coupling of the iodo- or ethynyl-substituted derivatives: A solution of the relevant iodo compound (200 to 300 mg scale) and the pyrene or perylene fragment (one mole equivalent) in benzene (25 mL) and triethylamine (5 mL) was degassed under argon for 30 min. Then, $[Pd(PPh_3)_4]$ (6 mol%) was added and the solution was stirred at 60 °C for 6 h. The solvent was removed by rotary evaporation. The residue was treated with water and extracted with dichloromethane. The organic phases were washed with water and brine, and dried over absorbent cotton. The solvent was removed by rotary evaporation. The resi-

due was purified by chromatography on silica gel, eluting with dichloromethane/petroleum ether (v/v 40:60) to give the desired derivatives as deep-red solids.

Compound BPY: Isolated yield 72%, 450 mg; ^{1}H NMR ($CDCl_3$): $\delta=8.62$ (d, $^3J=9.0$ Hz, 1H), 8.53 (d, $^3J=9.0$ Hz, 1H), 8.18–8.07 (8 line m, 6H), 7.57–7.55 (4 line m, 4H), 7.43 (d, $^3J=9.0$ Hz, 2H), 7.12 (d, $^3J=8.5$ Hz, 2H), 4.74 (s, 2H), 2.84 (s, 6H), 2.63 (s, 3H), 2.47 (q, $^3J=7.5$ Hz, 4H), 2.37 (s, 6H), 1.89 (brs, 1H), 1.11 ppm (t, $^3J=7.5$ Hz, 6H); ^{13}C {^{1}H} NMR ($CDCl_3$, 100 MHz): $\delta=151.9$, 139.8, 137.0, 134.6, 133.2, 132.6, 132.2, 131.9, 131.6, 131.3, 131.1, 130.2, 130.1, 129.9, 128.2, 128.0, 126.4, 126.1, 125.7, 125.2, 125.0, 124.1, 124.0, 121.8, 118.5, 117.6, 95.7, 93.1, 92.4, 89.6, 84.7, 52.0, 17.5, 17.3, 15.1, 14.7, 14.0 ppm; ^{11}B NMR (128.4 MHz, $CDCl_3$): $\delta=-9.69$ ppm (s); IR (KBr): νÜ=>=3065 (m), 2962 (m), 2934 (m), 2866 (m), 2167 (m), 2154 (m), 1612 (s), 1567 (s), 1489 (s), 1402 (m), 1387 (m), 1322 (m), 1183 (s), 1069 (m), 1061 (m), 1058 (m), 979 cm^{-1} (s); EI-MS: m/z (%): 886.2 (100) $[M]^+$; elemental analysis calcd (%) for $C_{55}H_{44}BION_2$ ($M_r=886.67$): C 74.50, H 5.00, N 3.16; found: C 74.21, H 4.82, N 2.93.

Compound BPP: Isolated yield 87%, 224 mg; ^{1}H NMR ($CDCl_3$): $\delta=8.66$ (d, $^3J=9.0$ Hz, 1H), 8.57 (d, $^3J=9.0$ Hz, 1H), 8.29–8.12 (15 line m, 11H), 7.74–7.69 (5 line m, 3H), 7.62–7.41 (18 line m, 11H), 4.74 (s, 2H), 2.88 (s, 6H), 2.68 (s, 3H), 2.50 (q, $^3J=7.5$ Hz, 4H), 2.40 (s, 6H), 1.85 (brs, 1H), 1.12 ppm (t, $^3J=7.5$ Hz, 6H); ^{13}C {^{1}H} NMR ($CDCl_3$, 100 MHz): $\delta=$ 152.0, 139.8, 134.7, 134.7, 132.7, 132.2, 131.9, 131.9, 131.7, 131.6, 131.5, 131.3, 131.2, 131.1, 131.0, 130.8, 130.2, 130.1, 129.9, 128.6, 128.5, 128.4, 128.2, 128.1, 127.3, 126.7, 126.6, 126.5, 126.2, 126.1, 125.8, 125.7, 125.2, 125.0, 124.2, 124.1, 121.8, 121.7, 120.9, 120.8, 120.6, 120.3, 119.7, 118.6, 95.7, 95.6, 92.6, 89.8, 84.9, 52.1, 17.5, 17.3, 15.1, 14.7, 14.0 ppm; ^{11}B NMR (128.4 MHz, $CDCl_3$): $\delta=-9.47$ ppm (s); IR (KBr): $\tilde{\nu}=3078$ (m), 2960 (m), 2929 (m), 2862 (m), 2165 (m), 2156 (m), 1616 (s), 1603 (s), 1567 (s), 1489 (s), 1412 (m), 1375 (m), 1329 (m), 1187 (s), 1079 (m), 1068 (m), 1063 (m), 993 cm^{-1} (s); EI-MS: m/z (%): 886.2 (100) $[M]^+$; elemental analysis calcd (%) for $C_{77}H_{55}BON_2$ ($M_r=1035.08$): C 89.35, H 5.36, N 2.71; found: C 89.05, H 5.09, N 2.56.

Compound BPPF: MnO_2 (88 mg, 1.00 mmol) and KOH (28 mg, 0.51 mmol) was added to a solution of BPP (112 mg, 0.108 mmol) in THF (10 mL). The mixture was stirred for 2 h and filtered. The solvent was removed by rotary evaporation. The residue was treated with water and extracted with dichloromethane. The organic extracts were washed with water and brine, and dried over absorbent cotton. The solvent was removed by rotary evaporation. Without further purification, the deprotected compound (108 mg, 0.107 mmol) was used in the cross-coupling reaction with **5**, using the general procedure described above, and afforded the target BPPF compound in 89% isolated yield (125 mg). ^{1}H NMR ($CDCl_3$): $\delta=8.75$ (d, $^3J=9.0$ Hz, 1H), 8.66 (d, $^3J=9.0$ Hz, 1H), 8.28–8.12 (13 line m, 11H), 7.78–7.35 (30 line m, 21H), 2.89 (s, 6H), 2.66 (s, 3H), 2.50 (q, $^3J=7.5$ Hz, 4H), 2.39 (s, 6H), 2.05 (t, $^3J=8.5$ Hz, 4H), 1.15–1.08 (6 line m, 8H), 1.12 ppm (t, $^3J=7.5$ Hz, 6H); ^{13}C {^{1}H} NMR ($CDCl_3$, 100 MHz): $\delta=151.9$, 151.1, 151.0, 141.7, 140.5, 139.8, 134.7, 134.6, 134.5, 132.7, 132.0, 131.9, 131.8, 131.7, 131.67, 131.62, 131.5, 131.3, 131.2, 131.1, 131.05, 131.03, 130.8, 130.7, 130.2, 129.99, 129.96, 128.6, 128.52, 128.50, 128.4, 128.2, 128.1, 128.0, 127.6, 127.3, 126.9, 126.7, 126.6, 126.4, 126.3, 126.2, 125.9, 125.8, 125.7, 125.2, 125.1, 124.3, 123.0, 121.8, 121.6, 120.9, 120.8, 120.6, 120.3, 120.0, 119.7, 118.7, 118.5, 118.4, 96.8, 95.7, 95.6, 95.0, 94.9, 89.7, 89.3, 88.6, 55.2, 40.3, 26.0, 23.1, 17.5, 17.3, 15.1, 14.7, 14.0; 13.9 ppm; ^{11}B NMR (128.4 MHz, $CDCl_3$): $\delta=-9.52$ ppm (s). IR (KBr): $\nu=3078$ (m), 3073 (m), 2960 (m), 2959 (m), 2929 (m), 2862 (m), 2167 (m), 2154 (m), 2153 (m), 2150 (m), 1618 (s), 1600 (s), 1563 (s), 1484 (s), 1416 (m), 1376 (m), 1332 (m), 1187 (s), 1185 (s), 1180 (s), 1079 (m), 1068 (m), 1063 (m), 997 cm^{-1} (s); EI-MS: m/z (%): 1280.5 (100) $[M]^+$; elemental analysis calcd (%) for $C_{97}H_{77}BN_2$ ($M_r=1281.47$): C 90.91, H 6.06, N 2.19; found: C 90.75, H 5.76, N 2.00.

Photophysical Studies All solvents were purchased as spectroscopic grade from Aldrich Chemicals, used as received, and were found to be free of fluorescent impurities. Absorption spectra were measured with a Hitachi U3310 spectrophotometer, corrected with a baseline and converted to molar absorption coefficient using the Beer–Lambert law, averaging over a series of dilute measurements of known concentration recorded at room temperature. Fluorescence spectra were measured with a fully corrected Jobin–Yvon Fluorolog tau-3 spectrometer for quantitative measurements and a Hitachi F-4500 fluorescence spectrometer for routine studies. Fluorescent measurements were obtained using optically dilute solutions having an absorbance less than or equal to 0.10 at the excitation wavelength. Fluorescence quantum yields were measured[56] at room temperature in CH_2Cl_2 relative to anthracene in ethanol ($\phi_F=0.27$; $\lambda_{EX}=280$ nm),[57] diphenylanthracene in cyclohexane ($\phi_F=0.90$; $\lambda_{EX}=$ 325 nm),[58] quinine sulfate in 0.5 M H_2SO_4 ($\phi_F=0.546$; $\lambda_{EX}=360$ nm),[59] Rhodamine 101 in ethanol ($\phi_F=1.0$; $\lambda_{EX}=450$ nm),[59] Rhodamine 6G in water ($\phi_F=0.95$; $\lambda_{EX}=488$ nm),[59] Fluorescein in 0.1 M NaOH ($\phi_F=0.95$; $\lambda_{EX}=496$ nm)[60] and Rhodamine B in water ($\phi_F=0.31$; $\lambda_{EX}=514$ nm).[59] Lifetime measurements were made using a PTI EasyLife spectrometer using Ludox in distilled water to determine the instrumental response function used for deconvolution. Excitation wavelengths of 310 nm (fluorene and pyrene), 440 nm (perylene and Bodipy), and 525 nm (Bodipy) were used. Fluorescence was isolated with a high radiance monochromator after passing through suitable cut-off filters. The resolution of this instrument is approximately 100 ps. The signal was averaged over a suitable time base and analysed by standard statistical methods. Additional time-resolved fluorescence studies were made with the Jobin–Yvon Fluorolog tau-3 spectrometer, which allows for better selection of excitation wavelengths and improves the temporal resolution to about 60 ps. Further improvement in temporal resolution was achieved using a high-intensity, ultra-short laser diode as excitation source and a cooled Hamamatsu R3809U-50 photo-detector used with a Becker & Hickl HFAC-26-01 preamplifier under time-correlated, single-photon counting methods. This set-up provided a wide range of excitation wavelengths. Low-temperature studies were recorded with an immersion Dewar held at 77 K. All solutions were purged with dried nitrogen before undertaking the measurement.

Spectral overlap integrals were measured using the appropriate reference compounds; structures are given in Scheme 2. These overlap integrals refer to the overlap of the absorption spectrum of the acceptor, recorded as molar absorption coefficient (ε_A) versus wavenumber ($\tilde{\nu}$), and the reduced fluorescence spectrum of the donor, also recorded in terms of wavenumber. The orientation factor was calculated for each pair of reactants using molecular dynamics simulations, as described previously. The respective center-to-center separation distances were derived using an optimised geometry obtained by molecular modeling. Molecular orbital calculations were made on energy-minimised conformations calculated by Gaussian 03[61] using the parameterised semi-empirical AM1 method[62] and checking for imaginary frequencies. Several starting geometries were sampled. Such AM1 calculations are far from definitive for boron-containing compounds but have been found to adequately model cyclic boron ethers.[63] Parameters for boron were taken from the literature.[64] These calculations were used to generate energy-minimised geometries and transition dipole moments for the dyes in vacuo. Molecular dynamics simulations (MDS) were performed with INSIGHT-II running on a Silicon Graphics O2 workstation. Structures were drawn in the Builder module and partial charges were assigned using the ESFF force field.[65] Energy minimisation was carried out with the Discover-3 module using the conjugate gradient method with a cut-off of 9.5 Å. The energy-minimised geometries were used as the starting points for the MDS studies. Each MDS run consisted of an initial 10 ps of equilibration using the velocity scaling method, followed by 100 ps of production dynamics. During this last stage, the temperature averaged 300 K with a standard deviation of 4.8 K. Data points were sampled each 10 fs of simulation time.

Acknowledgements

We thank the EPSRC (EP/D053080/1), the CNRS, the Université Louis Pasteur at Strasbourg and the University of Newcastle for financial support of this work. Dr. Sébastien Goeb is gratefully acknowledged for his expertise in carrying out the NMR studies and for preparing Figure 1.

[1] a) R. E. Blankenship, *Molecular Mechanism of Photosynthesis*, Blackwell Science, Oxford, **2002**; b) A. Freer, S. Prince, K. Sauer, M. Papiz, A. Hawthornwaiteless, G. McDermott, R. J. Cogdell, N. W. Isaacs, *Structure* **1996**, *4*, 449–462; c) C. J. Law, A. W. Roszak, J. Southall, A. T. Gardiner, N. W. Isaacs, R. J. Cogdell, *Mol. Membr. Biol.* **2004**, *21*, 183–191; d) J. Janusonis, L. Valkunas, D. Rutkauskas, R. van Grondellez, *Biophys. J.* **2007**, *94*, 1348–1358.

[2] a) D. Holten, D. F. Bocian, J. S. Lindsey, *Acc. Chem. Res.* **2002**, *35*, 57–69; b) A. L. Moore, D. Gust, T. A. Moore, *Actual. Chim.* **2007**, 50–56; c) T. A. Moore, A. L. Moore, D. Gust, *Phil. Trans. R. Soc.* **2002**, *357*, 9122–9129.

[3] a) M. Borgstrom, S. Ott, R. Lomoth, J. Bergquist, L. Hammarstrom, O. Johansson, *Inorg. Chem.* **2006**, *45*, 4820–4829; b) S. Fukuzumi, *Bull. Chem. Soc. Jpn.* **2006**, *79*, 177–195; c) G. Calzaferri, O. Bossarto, D. Bruhwiler, S. Huber, C. Leiggener, M. K. Van Veek, A. Z. Ruiz, *C. R. Chim.* **2006**, *9*, 214–225.

[4] a) C. Curutchet, B. Mennucci, G. D. Scholes, D. Beljonne, *J. Phys. Chem. B* **2008**, *112*, 3759–3766; b) B. Fückel, A. Kohn, M. E. Harding, G. Diezemann, G. Hinze, T. Basche, J. Gauss, *J. Chem. Phys.* **2008**, *128*, 074505; c) S. Jang, M. D. Newton, R. J. Silbey, *J. Phys. Chem. B* **2007**, *111*, 6807–6814; d) C. Didraga, V. A. Malyshev, J. Knoester, *J. Phys. Chem. B* **2006**, *110*, 18818–18827; e) E. K. L. Yeow, M. Ziolek, J. Karolczak, S. V. Shevyakov, A. E. Asato, A. Maciejewski, R. P. Steer, *J. Phys. Chem. A* **2004**, *108*, 10980–10988; f) K. F. Wong, B. Bagchi, P. J. Rossky, *J. Phys. Chem. A* **2004**, *108*, 5725–5763; g) K. Kilsa, J. Kajanus, J. Martensson, B. Albinsson, *J. Phys. Chem. B* **1999**, *103*, 7329–7339; h) S. H. Lin, W. Z. Xiao, W. Dietz, *Phys. Rev. E* **1993**, *47*, 3698–3706.

[5] a) A. Tsuda, A. Osuka, *Science* **2001**, *293*, 79–82; b) A. Tsuda, H. Furuta, A. Osuka, *J. Am. Chem. Soc.* **2001**, *123*, 10304–10321; c) H. S. Cho, D. H. Jeong, S. Cho, D. Kim, Y. Matsuzaki, K. Tanaka, A. Tsuda, A. Osuka, *J. Am. Chem. Soc.* **2002**, *124*, 14642–14654; d) X. Peng, N. Aratani, A. Takagi, T. Matsumoto, T. Kawai, I.-W. Hwang, T. K. Ahn, D. Kim, A. Osuka, *J. Am. Chem. Soc.* **2004**, *126*, 4468–4469; e) Y. Nakamura, N. Aratani, H. Shinokubo, A. Takagi, T. Kawai, T. Matsumoto, Z. S. Yoon, D. Y. Kim, T. K. Ahn, D. Kim, A. Muranaka, N. Kobayashi, A. Osuka, *J. Am. Chem. Soc.* **2006**, *128*, 4119–4127.

[6] a) T. V. Duncan, K. Susumu, L. E. Sinks, M. J. Therien, *J. Am. Chem. Soc.* **2006**, *128*, 9000–9001; b) A. Harriman, M. Hissler, O. Trompette, R. Ziessel, *J. Am. Chem. Soc.* **1999**, *121*, 2516–2525; c) A. Harriman, V. Heitz, M. Ebersole, H. Van Willigen, *J. Phys. Chem.* **1994**, *98*, 4982–4989; d) N. Mataga, H. Yao, T. Okada, Y. Kanda, A. Harriman, *Chem. Phys.* **1989**, *131*, 473–480; e) R. L. Brookfield, H. Ellul, A. Harriman, G. Porter, *J. Chem. Soc. Faraday Trans. 2* **1986**, *82*, 219–233.

[7] a) R. W. Wagner, J. S. Lindsey, *J. Am. Chem. Soc.* **1994**, *116*, 9759–9760; b) E. Hindin, R. S. Forties, R. S. Loewe, A. Ambroise, C. Kirmaier, D. F Bocian, J. S. Lindsey, D. Holten, R. S. Knox, *J. Phys. Chem. B* **2004**, *108*, 12821–12832; c) F. Li, S. I. Yang, Y. Ciringh, J. Seth, C. H. Martin III, D. L. Singh, D. Kim, R. R. Birge, D. F. Bocian, D. Holten, J. S. Lindsey, *J. Am. Chem. Soc.* **1998**, *120*, 10001–10017; d) R. K. Lammi, A. Amboise, T. Balasubramanian, R. W. Wagner, D. F. Bocian, D. Holten, J. S. Lindsey, *J. Am. Chem. Soc.* **2000**, *122*, 7579–7591; e) A. Ambroise, C. Kirmaier, R. W. Wagner, R. S. Loewe, D. F. Bocian, D. Holten, J. S. Lindsey, *J. Org. Chem.* **2002**, *67*, 3811–3826.

[8] a) P. A. Liddell, D. Kuciauskas, J. P. Sumida, B. Nash, D. Nguyen, A. L. Moore, T. A. Moore, D. Gust, *J. Am. Chem. Soc.* **1997**, *119*, 1400–1405; b) S. Rai, M. Ravikanth, *Chem. Phys. Lett.* **2008**, *453*, 250–255; c) J. Larsen, B. Bruggemann, T. Khoury, J. Sly, M. J. Crossley, V. Sundstrom, E. Alkesson, *J. Phys. Chem. A* **2007**, *111*, 10589–10597; d) M. Endo, M. Fujitsuka, T. Majima, *Chem. Eur. J.* **2007**, *13*, 8660–8666; e) Y. Shibano, M. Sasaki, Y. Kawanishi, Y. Araki, H. Tsuji, O. Ito, K. Tamao, *Chem. Lett.* **2007**, *36*, 1112–1113.

[9] M. R. Wasielewski, *J. Org. Chem.* **2006**, *71*, 5051–5066.

[10] a) Y. Nakamura, N. Aratani, A. Osuka, *Chem. Soc. Rev.* **2007**, *36*, 831–845; b) H. E. Song, C. Kirmaier, J. K. Schwartz, E. Hindin, L. H. Yu, D. F. Bocian, J. S. Lindsey, D. Holten, *J. Phys. Chem. B* **2006**, *110*, 19131–19139; c) A. Prodi, C. Chiorboli, F. Scandola, E. Lengo, E. Alessio, *ChemPhysChem* **2006**, *7*, 1514–1519.

[11] a) J. L. Sessler, B. Wang, A. Harriman, *J. Am. Chem. Soc.* **1995**, *117*, 704–714; b) A. Harriman, D. J. Magda, J. L. Sessler, *J. Phys. Chem.* **1991**, *95*, 1530–1532; c) A. M. Brun, A. Harriman, *J. Am. Chem. Soc.* **1994**, *116*, 10383–10393; d) F. J. M. Hoeben, M. Wolffs, J. Zhang, S. De Feyter, P. Leclere, A. P. H. J. Schenning, E. W. Meijer, *J. Am. Chem. Soc.* **2007**, *129*, 9819–9828; e) A. C. Benniston, *Phys. Chem. Chem. Phys.* **2007**, *9*, 5739–5747; f) L. A. Fendt, I. Bouamaied, S. Thoni, N. Amiot, E. Stulz, *J. Am. Chem. Soc.* **2007**, *129*, 15319–15329; g) V. Balzani, A. Credi, M. Venturi, *Chem. Eur. J.* **2008**, *14*, 26–39.

[12] a) M. P. Eng, T. Ljungdahl, J. Martensson, B. Albinsson, *J. Phys. Chem. B* **2006**, *110*, 6483–6491; b) I. V. Rubtsov, K. Susumu, G. I. Rubtsov, M. J. Therien, *J. Am. Chem. Soc.* **2003**, *125*, 2687–2693; c) T. V. Duncan, I. V. Rubtsov, H. T. Uyeda, M. J. Therien, *J. Am. Chem. Soc.* **2004**, *126*, 9474–9475; d) J. L. Sessler, V. L. Capuano, A. Harriman, *J. Am. Chem. Soc.* **1993**, *115*, 4618–4628; e) B. Albinsson, M. P. Eng, K. Pettersson, M. U. Winters, *Phys. Chem. Chem. Phys.* **2007**, *9*, 5847–5864.

[13] a) J. V. Caspar, E. M. Kober, B. P. Sullivan, T. J. Meyer, *J. Am. Chem. Soc.* **1982**, *104*, 630–632; b) V. Grosshenny, A. Harriman, M. Hissler, R. Ziessel, *J. Chem. Soc. Faraday Trans.* **1996**, *92*, 2223–2228; c) A. El-ghayoury, A. Harriman, A. Khatyr, R. Ziessel, *J. Phys. Chem. A* **2000**, *104*, 1512–1523; d) D. Gust, T. A. Moore, A. L. Moore, D. Kuciauskas, P. A. Liddel, B. D. Halbert, *J. Photochem. Photobiol. B* **1998**, *43*, 209–216; e) M. Galletta, F. Puntoriero, S. Campagna, C. Chiorboli, M. Quesada, S. Goeb, R. Ziessel, *J. Phys. Chem. A* **2006**, *110*, 4348–4358.

[14] R. P. Haugland, *Handbook of Molecular Probes and Research Products*, 9th ed., Molecular Probes, Eugene, OR, **2002**.

[15] a) R. Ziessel, G. Ulrich, A. Harriman, *New J. Chem.* **2007**, *31*, 496–501; b) G. Ulrich, R. Ziessel, A. Harriman, *Angew. Chem.* **2008**, *120*, 1202–1219; *Angew. Chem. Int. Ed.* **2008**, *47*, 1184–1201; c) R. Ziessel, *C. R. Chim.* **2007**, *10*, 622–629; d) A. Loudet, K. Burgess, *Chem. Rev.* **2007**, *107*, 4891–4932.

[16] a) T. Gareis, C. Huber, O. S. Wolfbeis, J. Daub, *Chem. Commun.* **1997**, 1717–1718; b) M. Kollmannsberger, K. Rurack, U. Resch-Genger, J. Daub, *J. Phys. Chem. A* **1998**, *102*, 10211–10220; c) K. Rurack, M. Kollmannsberger, U. Resch-Genger, J. Daub, *J. Am. Chem. Soc.* **2000**, *122*, 968–969; d) S. Y. Moon, N. R. Cha, Y. H. Kim, S.-K. Chang, *J. Org. Chem.* **2004**, *69*, 181–183; e) R. Ziessel, G. Ulrich, *Synlett* **2004**, 439–444; f) G. Ulrich, R. Ziessel, *J. Org. Chem.* **2004**, *69*, 2070–2083; g) G. Ulrich, R. Ziessel, *Tetrahedron Lett.* **2004**, *45*, 1949–1953; h) R. Ziessel, L. Bonardi, P. Retailleau, G. Ulrich, *J. Org. Chem.* **2006**, *71*, 3093–3102.

[17] I. V. Sazanovich, C. Kirmaier, E. Hindin, L. Yu, D. F. Bocian, J. S. Lindsey, D. Holten, *J. Am. Chem. Soc.* **2004**, *126*, 2664–2665.

[18] a) L. Bonardi, H. Kanaan, F. Camerel, P. Jolinat, P. Retailleau, R. Ziessel, *Adv. Funct. Mater.* **2008**, *18*, 401–413; b) J. O. Huh, Y. Do, M. H. Lee, *Organometallics* **2008**, *27*, 1022–1025.

[19] a) Y. Zhou, Y. Xiao, D. Li, M. Y. Fu, X. H. Qian, *J. Org. Chem.* **2008**, *73*, 1571–1574; b) T. A. Golovkova, D. V. Kozlov, D. C. Neckers, *J. Org. Chem.* **2005**, *70*, 5545–5549; c) S. Hattori, K. Ohkubo, Y. Urano, H. Sunahara, T. Nagano, Y. Wada, N. V. Tkachenko, H. Lemmetyinen, S. Fukuzumi, *J. Phys. Chem. B* **2005**, *109*, 15368–15375; d) D. Veldman, J. J. A. M. Bastiaansen, B. M. W. Langeveld-Voss, J. Sweelssen, M. M. Koetse, S. C. J. Meskers, R. A. J. Janssen, *Thin Solid Films* **2006**, *511*, 581–586; e) H. Sunahara, Y. Urano, H. Kojima, T. Nagano, *J. Am. Chem. Soc.* **2007**, *129*, 5597–5604.

[20] a) N. J. Bai, R. E. Pagano, *Biochemistry* **1997**, *36*, 8840–8848; b) R. C. A. Keller, J. R. Silvius, B. Dekruijff, *Biochem. Biophys. Res. Commun.* **1995**, *207*, 508–514; c) K. H. Huang, J. Y. Wu, W. S. Wu, C. C. Chang, H. L. Lee, T. C. Chang, *J. Lumin.* **2004**, *107*, 213–219.

[21] a) J. Y. Han, J. Jose, E. Mei, K. Burgess, *Angew. Chem.* **2007**, *119*, 1714–1717; *Angew. Chem. Int. Ed.* **2007**, *46*, 1684–1687; b) G. S. Jiao, L. H. Thoresen, T. G. Kim, W. C. Haaland, F. Gao, M. R. Topp, R. M. Hochstrasser, M. L. Metzker, K. Burgess, *Chem. Eur. J.* **2006**,

12, 7816–7826; c) T. G. Kim, J. C. Castro, A. Loudet, J. G.-S. Jiao, R. M. Hochstrasser, K. Burgess, M. R. Topp, *J. Phys. Chem. A* **2006**, *110*, 20–27; d) C.-W. Wan, A. Burghart, J. Chen, F. Bergström, L. B.-Å. Johansson, M. F. Wolford, T. G. Kim, M. R. Topp, R. M. Hochstrasser, K. Burgess, *Chem. Eur. J.* **2003**, *9*, 4430–4441; e) A. Burghart, L. H. Thorese, J. Che, K. Burgess, F. Bergström, L. B.-Å. Johansson, *Chem. Commun.* **2000**, 2203–2204; f) L. L. Li, J. Y. Han, B. Nguyen, K. Burgess, *J. Org. Chem.* **2008**, *73*, 1963–1970.

[22] R. Ziessel, C. Goze, G. Ulrich, M. Césario, P. Retailleau, A. Harriman, J. P. Rostron, *Chem. Eur. J.* **2005**, *11*, 7366–7378.

[23] a) J. Karolin, M. Fa, M. Wilczynska, T. Ny, L. B. Johansson, *Biophys. J.* **1998**, *74*, 11–21; b) G. Duvanel, N. Banerji, E. Vauthey, *J. Phys. Chem. A* **2007**, *111*, 5361–5369; c) X. Zhang, Y. Xiao, X. Qian, *Org. Lett.* **2008**, *10*, 29–32; d) S. Zrig, P. Rémy, B. Andrioletti, E. Rose, I. Asselberghs, K. Clays, *J. Org. Chem.* **2008**, *73*, 1563–1566; e) B. P. Wittmershaus, T. T. Baseler, G. T. Beaumont, Y. Z. Zhang, *J. Lumin.* **2002**, *96*, 107–118; f) M. Suzuki, Y. Ito, H. E. Savage, Y. Husimi, K. T. Douglas, *Chem. Lett.* **2003**, *32*, 306–307; g) S. Kalinin, L. B.-Å. Johansson, *J. Phys. Chem. B* **2004**, *108*, 3092–3097; h) M. D. Yilmaz, O. A. Bozdemir, E. U. Akkaya, *Org. Lett.* **2006**, *8*, 2871–2873.

[24] C. Goze, G. Ulrich, R. Ziessel, *J. Org. Chem.* **2007**, *72*, 313–322.

[25] a) A. Harriman, G. Izzet, R. Ziessel, *J. Am. Chem. Soc.* **2006**, *128*, 10868–10875; b) C. Goze, G. Ulrich, L. J. Mallon, B. D. Allen, A. Harriman, R. Ziessel, *J. Am. Chem. Soc.* **2006**, *128*, 10231–10239.

[26] A. Harriman, L. J. Mallon, S. Goeb, R. Ziessel, *Phys. Chem. Chem. Phys.* **2007**, *9*, 5199–5201.

[27] W. Qin, T. Rohand, M. Baruah, A. Stefan, M. Van der Auweraer, W. Dehaen, N. Boens, *Chem. Phys. Lett.* **2006**, *420*, 562–568.

[28] T. Rohand, J. Lycoops, S. Smout, E. Braeken, M. Sliwa, M. Van der Auweraer, W. Dehaen, W. M. De Borggraeve, N. Boens, *Photochem. Photobiol. Sci.* **2007**, *6*, 1061–1066.

[29] a) I. B. Berlman, *Handbook of Fluorescence Spectroscopy of Aromatic Molecules,* 2nd ed., Academic Press, New York, **1971**; b) D. A. Holden, W. A. Rendall, J. E. Guillet, *Ann. N. Y. Acad. Sci.* **1981**, *366*, 11–23; c) C. F. Wu, Y. L. Zheng, C. Szymanski, J. McNeil, *J. Phys. Chem. C* **2008**, *112*, 1772–1781.

[30] A. Harriman, M. Hissler, R. Ziessel, *Phys. Chem. Chem. Phys.* **1999**, *1*, 4203–4211.

[31] a) J. B. Birks, *Photophysics of Aromatic Molecules*, Wiley-Interscience, New York, **1970**; b) M. Belletête, J.-F. Morin, S. Beaupre, M. Leclerc, G. Durocher, *Synth. Met.* **2002**, *126*, 43–51; c) L. Pålsson, *Chem. Phys.* **2002**, *279*, 229–237.

[32] Molecular formulae for the reference compounds are given in Scheme 2.

[33] A. Harriman, A. Khatyr, R. Ziessel, A. C. Benniston, *Angew. Chem.* **2000**, *112*, 4457–4460; *Angew. Chem. Int. Ed.* **2000**, *39*, 4287–4291.

[34] D. L. Dexter, *J. Chem. Phys.* **1953**, *21*, 836–850.

[35] S. Saini, H. Singh, B. Bagchi, *J. Chem. Sci.* **2006**, *118*, 23–35.

[36] G. C. Claudio, E. R. Bittner, *J. Phys. Chem. A* **2003**, *107*, 7092–7100.

[37] a) K. F. Wong, B. Bagchi, P. J. Rossky, *J. Phys. Chem. A* **2004**, *108*, 5752–5763; b) I. H. Campbell, D. L. Smith, S. Tretiak, R. L. Martin, C. J. Neef, J. P. Ferraris, *Phys. Rev. B* **2002**, *65*, 085210.

[38] T. Förster, *Discuss. Faraday Soc.* **1959**, *27*, 7–23.

[39] C.-P. Hsu, G. R. Fleming, M. Head-Gordon, T. Head-Gordon, *J. Chem. Phys.* **2001**, *114*, 3065–3071.

[40] T. Sumi, *J. Phys. Chem. B* **1999**, *103*, 252–260.

[41] R. Baer, E. Rabani, *J. Chem. Phys.* **2008**, *128*, 184710.

[42] a) S. Jang, *J. Chem. Phys.* **2007**, *127*, 174710; b) R. D. Jenkins, D. L. Andrews, *Photochem. Photobiol. Sci.* **2003**, *2*, 130–135.

[43] G. A. Kumar, P. R. Biju, G. Jose, N. V. Unnikrishnan, *Mater. Chem. Phys.* **1999**, *60*, 247–255.

[44] B. Fückel, A. Köhn, M. E. Harding, G. Diezemann, G. Hinze, T. Basché, J. Gauss, *J. Chem. Phys.* **2008**, *128*, 074505.

[45] a) K. Pettersson, A. Kyrychenko, E. Ronnow, T. Ljungdahl, J. Martensson, B. Albinsson, *J. Phys. Chem. A* **2006**, *110*, 310–318; b) A. C. Benniston, A. Harriman, P. Y. Li, C. A. Sams, *J. Am. Chem. Soc.* **2005**, *127*, 2553–2564; c) M. P. Debreczeny, M. R. Wasielewski, S. Shinoda, A. Osuka, *J. Am. Chem. Soc.* **1997**, *119*, 6407–6414.

[46] a) "Delocalised Excitation and Excitation Transfer": T. Förster in *Modern Quantum Chemistry* (Ed.: O. Sinanoglu), Academic Press, New York, **1965**, pp. 93–137; b) S. Jang, M. D. Newton, R. J. Silbey, *Phys. Rev. Lett.* **2004**, *92*, 218301.

[47] B. P. Krueger, S. S. Lampoura, I. H. M. van Stokkum, E. Papagiannakis, J. M. Salverda, C. C. Gradinaru, D. Rutkauskas, R. G. Hiller, R. van Grondelle, *Biophys. J.* **2001**, *80*, 2843–2855.

[48] G. D. Scholes, R. D. Harcourt, *J. Chem. Phys.* **1996**, *104*, 5054–5061.

[49] R. H. Alden, E. Johnson, V. Nagarajan, W. W. Parson, C. J. Law, R. G. Cogdell, *J. Phys. Chem. B* **1997**, *101*, 4667–4680.

[50] S. T. Bailey, G. E. Lokey, M. S. Hanes, J. D. M. Shearer, J. B. McLafferty, G. T. Beaumont, T. T. Baseler, J. M. Layhue, D. R. Broussard, Y. Z. Zhang, B. P. Wittmershaus, *Sol. Energy Mater. Sol. Cells* **2007**, *91*, 67–75.

[51] a) S. A. Vail, P. J. Krawczuk, D. M. Guldi, A. Palkar, L. Echegoyen, J. P. C. Tome, M. A. Fazio, D. I. Schuster, *Chem. Eur. J.* **2005**, *11*, 3375–3388; b) D. P. Arnold, G. A. Heath, D. A. James, *New J. Chem.* **1998**, *22*, 1377–1387; c) D. P. Arnold, D. Manno, G. Micocci, A. Serra, A. Tepore, L. Valli, *Langmuir* **1997**, *13*, 5951–5956; d) A. Harriman, R. Ziessel, *Chem. Commun.* **1996**, 1707–1716.

[52] M. Shah, K. Thangaraj, M. L. Soong, L. Wolford, J. H. Boyer, I. R. Politzer, T. G. Pavlopoulos, *Heteroat. Chem.* **1990**, *1*, 389–400.

[53] R. Ziessel, S. Diring, *Tetrahedron Lett.* **2006**, *47*, 4687–4692.

[54] M. Inouye, Y. Hyodo, H. Nakazumi, *J. Org. Chem.* **1999**, *64*, 2704–2710.

[55] H.-J. Cho, D.-H. Hwang, J.-I. Lee, Y.-K. Jung, J.-H. Park, J. Lee, S.-K. Lee, H.-K. Shim, *Chem. Mater.* **2006**, *18*, 3780–3787.

[56] A. K. Gaigalas, L. Wang, *J. Res. Natl. Inst. Stand. Technol.* **2008**, *113*, 17–28.

[57] D. F. Eaton, *Pure Appl. Chem.* **1988**, *60*, 1107–1114.

[58] S. R. Meech, D. Phillips, *J. Photochem.* **1983**, *23*, 193–217.

[59] D. Magde, G. E. Rojas, P. Seybold, *Photochem. Photobiol.* **1999**, *70*, 737–741.

[60] J. R. Lakowicz, *Principles of Fluorescence Spectroscopy*, 2nd ed., Kluwer Academic–Plenum, New York, **1999**.

[61] Gaussian 03, Revision C.02, M. J. Frisch, G. W. Trucks, H. B. Schlegel, G. E. Scuseria, M. A. Robb, J. R. Cheeseman, J. A. Montgomery Jr., T. Vreven, K. N. Kudin, J. C. Burant, J. M. Millam, S. S. Iyengar, J. Tomasi, V. Barone, B. Mennucci, M. Cossi, G. Scalmani, N. Rega, G. A. Petersson, H. Nakatsuji, M. Hada, M. Ehara, K. Toyota, R. Fukuda, J. Hasegawa, M. Ishida, T. Nakajima, Y. Honda, O. Kitao, H. Nakai, M. Klene, X. Li, J. E. Knox, H. P. Hratchian, J. B. Cross, V. Bakken, C. Adamo, J. Jaramillo, R. Gomperts, R. E. Stratmann, O. Yazyev, A. J. Austin, R. Cammi, C. Pomelli, J. W. Ochterski, P. Y. Ayala, K. Morokuma, G. A. Voth, P. Salvador, J. J. Dannenberg, V. G. Zakrzewski, S. Dapprich, A. D. Daniels, M. C. Strain, O. Farkas, D. K. Malick, A. D. Rabuck, K. Raghavachari, J. B. Foresman, J. V. Ortiz, Q. Cui, A. G. Baboul, S. Clifford, J. Cioslowski, B. B. Stefanov, G. Liu, A. Liashenko, P. Piskorz, I. Komaromi, R. L. Martin, D. J. Fox, T. Keith, M. A. Al-Laham, C. Y. Peng, A. Nanayakkara, M. Challacombe, P. M. W. Gill, B. Johnson, W. Chen, M. W. Wong, C. Gonzalez, J. A. Pople, Gaussian, Inc., Wallingford CT, **2004**.

[62] a) M. J. S. Dewar, C. H. Reynolds, *J. Comput. Chem.* **1986**, *7*, 140–143; b) M. J. S. Dewar, E. G. Zoebisch, E. F. Healy, *J. Am. Chem. Soc.* **1985**, *107*, 3902–3909; c) M. J. S. Dewar, H. S. Rzepa, *J. Am. Chem. Soc.* **1978**, *100*, 3607–3607.

[63] V. V. Kuznetsov, *J. Struct. Chem.* **2001**, *42*, 494–499.

[64] M. J. S. Dewar, C. Jie, E. G. Zoebisch, *Organometallics* **1988**, *7*, 513–521.

[65] Discover3 User Guide, September 1996, Molecular Simulations, San Diego, **1996**.

Received: July 8, 2008
Published online: November 12, 2008

